Predicting Soil Organic Carbon Stock Using Profile Depth Distribution Functions and Ordinary Kriging

Umakant Mishra*
Rattan Lal
Carbon Management and Sequestration Center
School of Environment and Natural Resources
Ohio State Univ.
2021 Coffey Rd.
Columbus, OH 43210

Brian Slater
Frank Calhoun
School of Environment and Natural Resources
Ohio State Univ.
2021 Coffey Rd.
Columbus, OH 43210

Desheng Liu
Dep. of Geography and Dep. of Statistics
Ohio State Univ.
1036 Derby Hall
154 N Oval Mall
Columbus, OH 43210

Marc Van Meirvenne
Dep. of Soil Management and Soil Care
Ghent Univ.
Coupure 653
9000 Ghent, Belgium

The objective of this study was to predict and map SOC stocks at different depth intervals within the upper 1-m depth using profile depth distribution functions and ordinary kriging. These approaches were tested for the state of Indiana as a case study. A total of 464 pedons representing 204 soil series was obtained from the National Soil Survey Center database. Another 48 soil profile samples were collected to better represent the heterogeneity of the environmental variables. Two methods were used to model the depth distribution of the SOC stocks using negative exponential profile depth functions. In Procedure A, the functions to describe the depth distribution of volumetric C content for each soil profile were fitted using nonlinear least squares. In Procedure B, the exponential functions were fitted to describe the depth distribution of the cumulative SOC stocks. The parameters of the functions were interpolated for the entire study area using ordinary kriging on 81% of the data points (n = 414). The integral of the exponential function up to the desired depth was used to predict SOC stocks within the 0- to 1-, 0- to 0.5-, and 0.5- to 1-m depth intervals. These estimates were validated using the remaining 19% (n = 98) of the data. Procedure B showed a higher prediction accuracy for all depths, with higher r and lower RMSE values. The highest prediction accuracy (r = 0.75, RMSE = 2.89 kg m^{-2}) was obtained for SOC stocks in the 0- to 0.5-m depth interval. Using Procedure B, SOC stocks within the top 1 m of Indiana soils were estimated to be 0.90 Pg C.

Abbreviations: MEE, mean estimation error; OK, ordinary kriging; SOC, soil organic carbon.

The SOC pool is an important component in the global C cycle, as it contains more C than the atmosphere and biosphere together (Batjes, 1996; Grace, 2004). Soil organic C plays an important role in enhancing crop production and mitigating the net rate of greenhouse gas emissions (Lal et al., 1995; Post and Kwon, 2000). The risk of global warming and interest in adoption of the Kyoto Protocol have increased the attention of the scientific community on SOC stocks in the terrestrial ecosystems (Intergovernmental Panel on Climate Change, 2007). Precise measurement of the SOC stocks and verification of the amount of C sequestered in the soil are among the critical factors in implementing C trading programs. Similarly, estimates of the spatial distribution of SOC stocks are necessary to quantify the SOC sink capacity of soils. Soil organic C maps showing the sink capacity at various scales are necessary to design an effective C sequestration program. Therefore, obtaining an accurate map is important, as both the rate of change in SOC and the sink capacity depend on the initial SOC stock. Estimates of SOC stocks at larger spatial scales across different soil depth intervals are limited by time and cost constraints (Sleutel et al., 2003: Goidts and van Wesemael, 2007). Therefore, digital SOC mapping representing SOC stocks at different spatial scales such as plot, watershed, county, regional, and national levels are important.

The magnitude of SOC stocks at a location depends on a range of factors such as the soil type, land use, annual input of biomass C, and the severity of degradation. Therefore, several approaches and techniques are needed to develop a reliable estimate of SOC stocks at different spatial scales (Van Meirvenne et al., 1996; Post et al., 2001; Lal, 2004). Simbahan

Soil Sci. Soc. Am. J. 73:614-621
doi:10.2136/sssaj2007.0410
Received 29 Nov. 2007.
*Corresponding author (mishra.24@osu.edu).

and Dobermann (2006) reported the need for further research in using secondary information to map SOC stocks at different scales. Quantifying SOC stocks at different spatial scales in a cost-effective manner is a priority research topic for soil scientists.

Previous studies have estimated SOC stocks at global (Post et al., 1990; Eswaran et al., 1993), national (Kern, 1994; Guo et al., 2006a), state (Amichev and Galbraith, 2004; Tan et al., 2004), and regional (Homann et al., 1998; Yu et al., 2007) scales. These estimates were based on the measure-and-multiply approach, where the study area is separated into different strata and the SOC measurements within each stratum are multiplied by the area of that stratum. Although the method is useful for estimating SOC stocks under different ecosystems, the estimates thus obtained do not account for spatial variability due to soil heterogeneity within each stratum (Thompson and Kolka, 2005; Rasmussen, 2006). The errors associated with assigning a mean SOC content to mapping units from a small number of samples can be an important source of discrepancy (Meersmans et al., 2008).

Alternatively, studies showing the spatial variability of SOC stocks have been conducted at plot (Simbahan et al., 2006), watershed (Minasny et al., 2006), and regional (Meersmans et al., 2008) scales. These studies used a variety of techniques such as geostatistics, artificial neural networks, and multiple regression in SOC stock mapping. These techniques were useful, as they showed the spatial variability of SOC stocks and their associated uncertainty; however, no studies have been conducted to quantify SOC stock variability at different depth intervals using profile depth distribution functions and geostatistics at regional scales. Thus, the objective of this study was to predict and map SOC stocks at different depth intervals within the upper 1-m depth on a state scale using profile depth distribution functions and ordinary kriging. The Midwest Regional Carbon Sequestration Partnership (MRCSP) project funded by the U.S. Department of Energy to assess the potential of C sequestration and strategies to mitigate CO_2 emissions provided an opportunity to conduct this study at a larger spatial scale. Therefore, as a case study, the entire state of Indiana was selected. Indiana is one of the seven states in the MRCSP project. The hypothesis tested was that if the variability in environmental variables that affect soil development can be captured through soil samples, it is possible to predict the SOC stock reliably and credibly. The environmental variables of elevation, climatic factors (temperature and precipitation), and land use were included in this study.

MATERIALS AND METHODS

Study Area and Data Sources

The study was conducted in Indiana, with central coordinates 39°53.7′ N and 86°16.0′ W. The study area is 94,319 km^2, with elevation ranging from 96 to 380 m above mean sea level. The highest elevated area is located in the southeast portion of the state. Similarly, areas with the lowest elevations are located in the northwest and southwest corners of the state. The long-term (1975–2005) average annual temperature ranged from 8.5 to 14°C and the long-term precipitation ranged from 860 to 1270 mm. Both the temperature and precipitation increased gradually from the northern to the southern part of the state. The soils of study area were classified as Alfisols, Mollisols, Inceptisols, Entisols, Ultisols, and Histosols, with about 350 identified soil series. A total of 464 georeferenced soil profile data representing 204 soil series were extracted from the NSSC database (National Soil Survey Laboratory, 2006). These soil samples were collected within a 15-yr span from 1975 to 1990. A digital elevation model (DEM), with 30-m pixel resolution, and land cover data of similar resolution were extracted for the study area from the USGS database (Multi-Resolution Land Characteristics Consortium, 2006). The land cover map of Indiana had 16 land classes. Major land classes identified were: cropland, forest, grassland, water, developed land, and wetland.

Climate data, such as long-term point observations of mean annual air temperature (MAAT) and mean annual precipitation (MAP), were obtained from the National Climatic Data Center database. Among the collected environmental variables, elevation showed significant correlations with MAAT (r = 0.72, P < 0.001) and MAP (r = 0.60, P < 0.001) data. Various studies have shown that when sufficient correlation exists between a variable and environmental parameters, kriging combined with regression on these parameters is both easy to implement and sufficiently accurate (Odeh et al., 1994; McBratney et al., 2000; Van Meirvenne and Van Cleemput, 2005). Therefore, regression kriging (Hengl et al., 2004) was used to obtain a continuous surface of weather parameters for the study area. Linear regression of MAAT (67 data points) and MAP (84 data points) with elevation data was performed for the observation sites and the regression equation was used to predict the precipitation and temperature for the entire study area. Omnidirectional variograms were computed from the residuals and kriged residual maps of both parameters were added to the regression prediction maps to obtain the regression kriged prediction (data not shown). The MAAT and MAP maps were developed at a similar spatial resolution (30 m) to the DEM and land cover maps, and all four environmental variables were used to guide the collection of additional soil samples across the study area.

Systematic (grid) sampling has been used extensively in geostatistical mapping (Baxter and Oliver, 2005; Minasny et al., 2006; Simbahan et al., 2006). This sampling strategy may not be practical for regional-scale studies, however, due to several reasons such as inaccessible areas, already available preliminary information that makes a regular grid superfluous, and edge effects (van Groenigen, 2000). Therefore, the variability of environmental parameters that are expected to affect the SOC was sampled. For this purpose, soil samples were overlaid on the maps of elevation, land use, temperature, and precipitation. After observing the distribution of soil samples, 48 additional soil sample points were identified interactively in the geographic information system environment to better represent the heterogeneity of the environmental variables in the study area. Soil samples from the identified locations were collected during mid-March to late April 2006. The samples were obtained from soil pits at 0- to 5-, 5- to 10-, 10- to 30-, 30- to 50-, and >50-cm depths. A hammer-driven core sampler was used to collect the soil cores (5.4-cm diameter and 6-cm depth) for bulk density (ρ_b) measurements and a bulk soil sample of about 1 kg was collected for SOC measurements. Samples were sealed in plastic bags and transported to the laboratory. A total of 98 samples were randomly selected from the whole data set, dividing the data set (n = 512) into calibration (n = 414) and validation data sets (n = 98). This was done using the Create Subset function of Geostatistical Analyst in ArcGIS 9.2 (ESRI, Redlands, CA). Figure 1 shows the spatial distribution of the calibration and validation sites of the SOC samples across the study area.

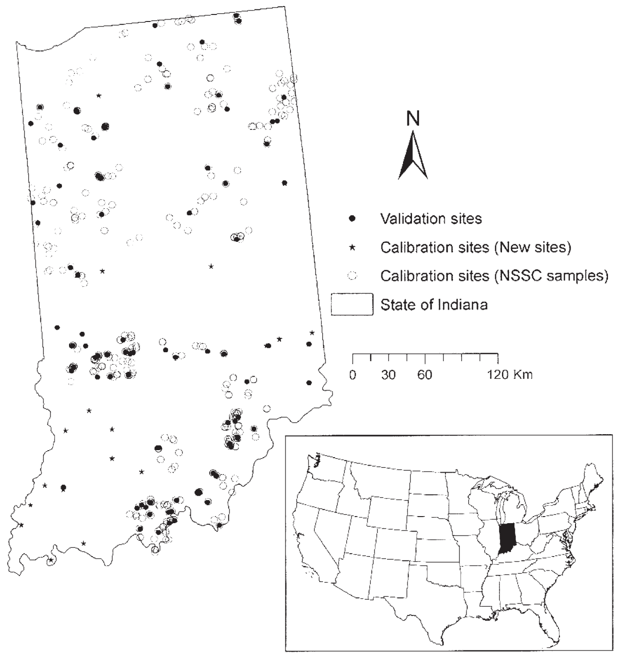

Fig. 1. The state of Indiana, showing the distribution of calibration (*n* = 414) and validation sites (*n* = 98) and the location of the study site within United States.

Data Modeling and Soil Organic Carbon Stock Prediction

The collected additional soil samples were analyzed for C concentration by the dry combustion method (900°C) using a C-N analyzer (Vario Max, Elementar Analysensysteme, Hanau, Germany; Nelson and Sommers, 1996). Dry ρ_b was calculated using the core method (Blake and Hartge, 1986). The SOC concentration on a mass basis (C_m, kg kg^{-1}) was converted to a volumetric basis (C_v, kg m^{-3}) by using the ρ_b (kg m^{-3}):

$$C_v = C_m \rho_b \quad [1]$$

Soil ρ_b values were not available for all the pedons in the data set, thus ρ_b was predicted from the soil texture, SOC concentration, and depth of the horizons by using the pedotransfer function developed by Calhoun et al. (2001) (R^2 = 0.56):

$$\begin{aligned}\rho_b = &1.594 - 0.084\text{SOC} - 0.0018\text{Silt} \\ &- 0.0020\text{Clay-free silt} + 0.0001\text{Clay(Sand)} \\ &- 0.0466\text{Clay/Silt} + 0.0008\text{Depth}\end{aligned} \quad [2]$$

where clay-free silt is the percentage of silt in the silt and sand fractions only, excluding the clay fraction. This model gave unrealistic predictions for the horizons with high SOC concentrations. Therefore, the pedotransfer function developed by Adams (1973) was used for horizons with a SOC concentration >6%:

$$\rho_b = \frac{100}{(\text{SOM}/\rho_{om}) + (100 - \text{SOM}/\rho_{mn})} \quad [3]$$

where SOM is the percentage by weight of organic matter, ρ_{om} is the average bulk density of organic matter (224 kg m^{-3}), and ρ_{mn} is the bulk density of the mineral matter.

The distribution of SOC concentration with depth is essential information for estimating SOC stocks. In many cases, the SOC concentration decreased exponentially with an increase in soil depth. Among the various models that have been proposed, the exponential C depth model is the most widely accepted (Mestdagh et al., 2004; Zinn et al., 2005; Minasny et al., 2006). The following negative exponential function was fitted for each sample point in the calibration data set from the surface to 1-m depth:

$$C = a\exp(-bD) \quad [4]$$

where C is the SOC concentration (kg m^{-3} in Procedure A and kg m^{-2} in Procedure B), D is the absolute depth (m), and a and b are the parameters of the exponential function. The integral of the exponential equation down to the desired depth was used to calculate the SOC stock at a particular location:

$$C_s = \int_0^Z a\exp(-bD) \quad [5]$$

where C_s is the C stock (kg m^{-2}) down to the desired depth (D) in the soil profile. Solving the integral equation with respect to depth from the surface to D yields

$$C_s = -\frac{a}{b}\left[\exp(-bD) - 1\right] \quad [6]$$

Table 1. Moran's index (*I*) statistic showing spatial autocorrelation in the parameters.

Variable	Procedure A		Procedure B	
	Moran's *I*	*P* value	Moran's *I*	*P* value
Parameter *a*	0.1229	0.0020	0.1126	0.0010
Parameter *b*	0.0948	0.0010	0.1698	0.0010

Two different methods were used in modeling the depth distribution of the SOC concentration. In Procedure A, the exponential functions were fitted to describe the depth distribution of C_v for each soil profile using a nonlinear least squares procedure. The C_v was calculated using Eq. [1] for each horizon of the soil profiles down to 1-m depth. In Procedure B, the exponential functions were fitted to describe the depth distribution of the cumulative SOC stock in individual soil profiles. The cumulative SOC stock was calculated for the incremental horizon or layer depths in each profile using Eq. [7]

$$C_s = \rho_b C_m D \quad [7]$$

where C_s is the SOC stock (kg m^{-2}), ρ_b is the bulk density (kg m^{-3}), C_m is the SOC concentration (kg kg^{-1}), and D is the soil depth (m).

The parameters of the exponential functions from both procedures were tested for the presence of spatial autocorrelation using Moran's Index (I) (Moran, 1950). Moran's I showed significant spatial autocorrelation in the parameters (Table 1). This led to the use of an interpolation technique that capitalizes on the spatial autocorrelation present in the calculated parameters. Therefore, a geostatistical technique was used to interpolate the parameters across the study area. The obtained parameters were not significantly correlated with the environmental variables. The highest Pearson's correlation coefficient (r) value of 0.28 was observed between parameter a (using Procedure A) and precipitation. Therefore, secondary information could not be incorporated in mapping the parameters and ordinary kriging (OK) was used for the interpolation. Ordinary kriging is the most common type of kriging in practice. It assumes local stationarity of the mean of the variable under investigation.

Ordinary kriging is used to estimate the value of a random variable, Z, at one or more unsampled points or across larger blocks from a sparse data set. The kriging estimate of variable Z at point x_0, $\hat{Z}(x_0)$, is a linear weighted sum of n observations surrounding the estimate (Eq. [8]):

$$\hat{Z}(x_0)=\sum_{i=1}^{n}\lambda_i z(x_i) \qquad [8]$$

where λ_i are the weights and $z(x_i)$ is the known value of variable Z at sampling site x_i.

The n weights are then chosen such that the estimate is unbiased and has minimum kriging variance. The unbiasedness is ensured when the sum of n weights are made equal to 1 (Eq. [9]):

$$\sum_{i=1}^{n}\lambda_i = 1 \qquad [9]$$

A detailed theoretical description of the kriging algorithms was provided by Webster and Oliver (2001).

The interpolated maps of the parameters were then used to solve Eq. [6] to get the SOC stocks for the entire study area using Procedure A. In Procedure B, the obtained maps of the parameters were used in Eq. [4] to obtain the C stock across the desired depth intervals.

The SOC stocks for entire state of Indiana were estimated using the predicted raster map of SOC stocks (0–1-m depth). For this purpose, the raster map was multiplied by the pixel area to convert the SOC stocks (kg m^{-2}) to a mass basis (kg) for each pixel. The individual pixels were then summed to get the SOC stocks for the entire state.

Validation of Predicted Soil Organic Carbon Stock Estimates

The uncertainty of the SOC stock maps was assessed using the independent validation data set. For the validation data set, the SOC stock was estimated in each profile by summing the C stocks of each horizon from the surface to the depth of 1 m using

$$C_s=\sum_{j=1}^{n}(C_m\rho_b)D \qquad [10]$$

where C_s is the C stock (kg m^{-2}), j is the soil horizon (e.g., 1, 2, 3…, n), C_m is the C concentration on a mass basis (kg kg^{-1}), ρ_b is the soil bulk density corrected for rock fragments (kg m^{-3}), and D is the thickness of each horizon (m).

From the predicted SOC map, SOC stock values were extracted for the validation points. The obtained values of observed and predicted C stocks were interpreted by calculating different validation indices, such as r between the observed and predicted SOC values, the mean estimation error (MEE), the RMSE, and the relative improvement (RI):

$$\mathrm{MEE}=\frac{1}{n}\sum_{i=1}^{n}\left[\hat{C}_s(x_i)-C_s(x_i)\right] \qquad [11]$$

$$\mathrm{RMSE}=\sqrt{\frac{1}{n}\sum_{i=1}^{n}\left[\hat{C}_s(x_i)-C_s(x_i)\right]^2} \qquad [12]$$

where $C_s(x_i)$ is the measured C concentration, $\hat{C}_s(x_i)$ is the estimated C concentration, and n is the number of validated observations. The MEE represents the bias of the predictions and the RMSE represents the average error of prediction. These values should approach zero for an optimal prediction. The relative improvement (%) of one method over the other was calculated using

Table 2. Summary statistics of soil organic *C* stock data (*n* = 512 samples).

Parameter	Value
Mean, kg m^{-2}	9.50
Minimum, kg m^{-2}	1.57
Maximum, kg m^{-2}	125.2
Median, kg m^{-2}	7.17
Variance, (kg $m^{-2})^2$	100.68
Coefficient of skewness	7.72
Coefficient of kurtosis	78.5

$$\mathrm{RI}=\frac{\mathrm{RMSE_A}-\mathrm{RMSE_B}}{\mathrm{RMSE_A}}100 \qquad [13]$$

where $\mathrm{RMSE_A}$ and $\mathrm{RMSE_B}$ are the root mean square errors of Procedures A and B, respectively.

The quality of prediction was also tested by examining the 1:1 relationship between the observed and predicted SOC stocks at different depth intervals. The t-test (Devore and Peck, 1993) was used to test the hypothesis that the slope of the regression line equals 1.

RESULTS AND DISCUSSION

Exploratory Data Analysis

The summary statistics of the SOC stock data show a unimodal but positively skewed distribution (coefficient of skewness = 7.72) around a mean of 9.50 kg m^{-2} ranging between 1.6 and 125.2 kg m^{-2} (Table 2). The higher values were observed mainly in the northern part of the state. The large value of the coefficient of kurtosis (78.5) indicates that there are fewer observations situated around the mean value of SOC stock than for a normal distribution. This is mainly due to the large areas of Alfisols and Inceptisols, which usually have lower SOC stocks in comparison to other soil types (Mollisols and Histosols). The large variance, 100.7 (kg $m^{-2})^2$, is due to the many different soil types with strongly differing SOC contents (Entisols, Inceptisols, to Histosols). Extreme SOC values such as those >44.5 kg m^{-2} are the major influencing points in the data set. These values are typical for the Histosols found in the study area, so they should not be considered as outliers.

Soil Organic Carbon Modeling with Depth

Exponential functions (Eq. [4]) were fitted to the SOC concentrations of the horizons in each soil profile down to 1-m depth. The fitted exponential functions showed a mean value of r = 0.95 and a RMSE = 4.98 kg m^{-3} between the observed and fitted SOC stocks for all the soil profiles using Procedure A. In Procedure B, the fitted exponential function showed a mean value of r = 0.98 and a RMSE = 1.03 kg m^{-2} between the observed and fitted SOC storage for all profiles. These results indicate that both of the methods fitted the data very well. The higher r and lower RMSE values suggest, however, that the exponential function fitting method of Procedure B (with cumulative SOC stock values) will result in lower errors in predicting the SOC stocks than Procedure A. The data in Fig. 2 show the relationship between the observed and fitted exponential function C values using both methods.

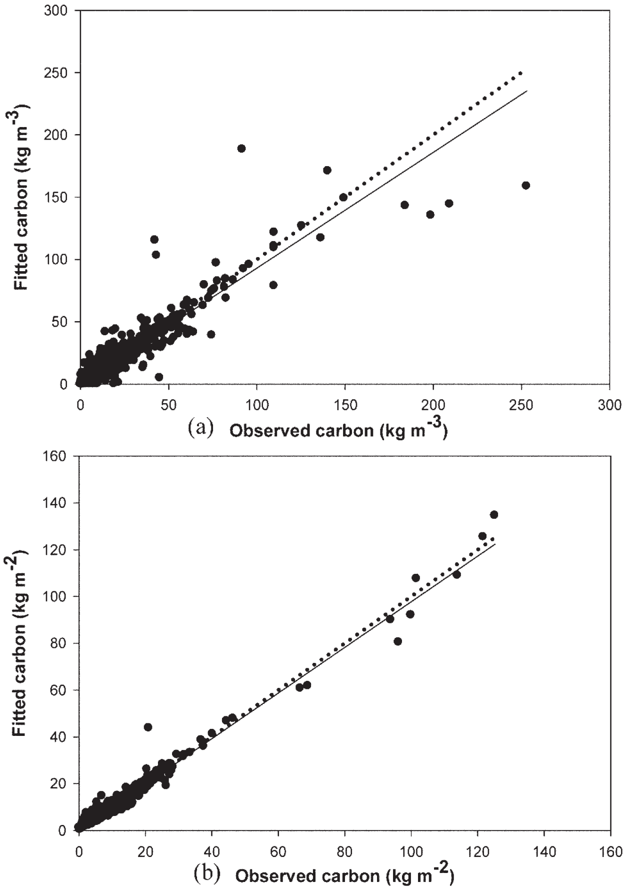

Fig. 2. Observed and fitted exponential depth function soil organic C stocks by (a) Procedure A and (b) Procedure B (*n* = 414 calibration sites); dashed line is the 1:1 line.

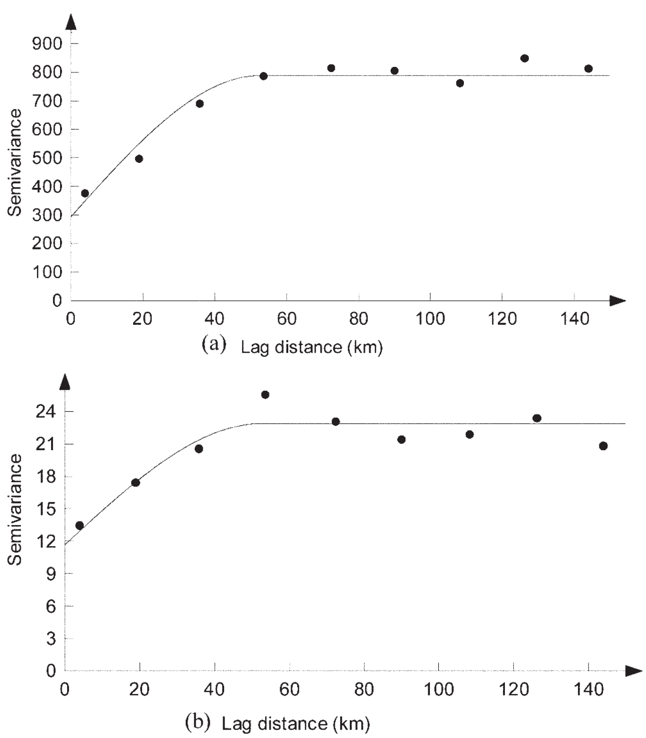

Fig. 3. Experimental variograms and fitted models used for interpolation of parameters (a) *a* and (b) *b* using Procedure A; symbols represent the experimental semivariances and the solid line is the fitted model.

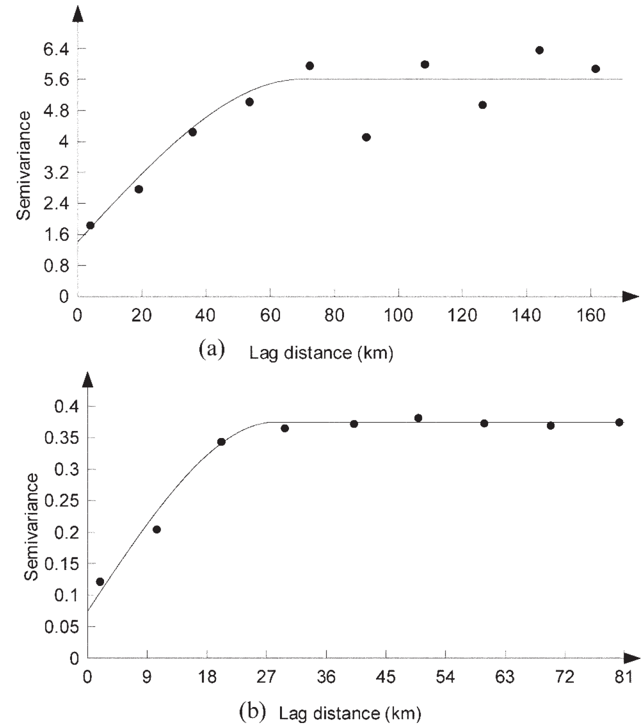

Fig. 4. Experimental variograms and fitted models used for interpolation of parameters (a) *a* and (b) *b* using Procedure B; symbols represent the experimental semivariances and the solid line is the fitted model.

Spatial Interpolation of the Parameters of the Exponential Functions

The observation sites of the *a* and *b* parameters were used to compute the experimental variograms. The experimental variogram values were fitted with omnidirectional spherical models (Webster and Oliver, 2001), as anisotropy was not observed in the variogram surface. Figures 3 and 4 show the experimental variograms (symbols) with the fitted models (solid lines) of the parameters obtained from both methods. The model parameters of the variograms are given in Table 3.

The fitted variograms show similar trends of spatial variation for both parameters in Procedure A. In Procedure B, the variograms suggested a shorter spatial dependence (smaller range) in parameter *a* than parameter *b*. The parameters of the exponential functions fitted according to both procedures were then interpolated to a 100- by 100-m grid using OK across the entire study area. The diameter of the interpolation window was kept within the range of the variogram models.

Prediction and Validation of the Soil Organic Carbon Stock

The interpolated maps of the parameters were used to predict and map the SOC stocks for the whole study area for different depth intervals: 0 to 1.0 m, the surface soil (0–0.50 m), and the subsoil (0.50–1.0 m) (Fig. 5). All three maps indicated higher SOC stocks in the northern part than the southern part of the state. In general, the spatial distribution of the SOC stocks is similar in both surface soils and subsoils, but the subsoil map shows a few locations where the SOC stocks are higher in the subsoil than in the surface layer. Figure 6 shows both the areas where the surface soil has the highest SOC stock and the reverse. In most of the study area, the SOC is mainly stored in the topsoil, but apparently in a few areas there is more SOC stored in the subsoil. Areas with high subsoil SOC stocks are located in regions with low gradients (<5% slope angle) and high percentages of poorly drained soils. The data in Fig. 7 show the profile depth distributions of the SOC stocks of the pedons that had higher SOC stocks in the subsoil.

The data in Table 4 show the validation indices of the predicted SOC stocks at different depth intervals for both methods. In the 0- to 1-m depth, the MEE is close to zero with both methods, which confirms the unbiasedness of OK. A higher r and a lower RMSE suggest that the exponential function fitting method of Procedure B produces less error in predicting the SOC stocks. Similarly, SOC stocks were predicted with lower errors by Procedure B in both the surface soil and subsoil. Both methods resulted in higher prediction errors when estimating the SOC stocks in the subsoil than the surface soil layer. The RI estimates showed that the SOC stock predictions improved at all depth intervals by using Procedure B over Procedure A. The RMSE decreased by 5% in the 0- to 1-m depth, 11.6% in the topsoil, and 1.5% in the subsoil. This RI in Procedure B resulted because the cumulative SOC stock increases with depth, whereas the SOC concentration does not always decrease with depth (down to 1 m), for example in Histosols and Fluvents that are present in the study area.

The data in Table 5 show the results of the t-test used to test the hypothesis that the slope of the regression line between the measured and predicted SOC stocks equals 1. The results indicate that in 0 to 1 m and the subsoil, the slope of the regression line of Procedure B is not significantly different than 1, suggesting more accurate predictions of SOC stocks in comparison to Procedure A. In the topsoil, however, the slopes from both methods are significantly different than 1, which means SOC stocks are either under- or overpredicted.

Distribution of Soil Organic Carbon Stock

The SOC map obtained by Procedure B was used to describe the spatial variation in SOC stocks across the study area. Indiana is divided into nine Major Land Resource Areas (MLRAs), namely, 98, 99, 110, 111, 114, 115, 120, 121, and 122. The MLRA is a geographical unit that contains similar patterns of climate, soils, water resources, and land uses (Soil Conservation Service, 1981). With regard to the physiographic distribution of SOC stocks, MLRAs 98, 99, 110, and 111 had higher SOC stocks. These MLRAs are located in the northern part of the state and are characterized by low gradients (<5%) and high percentages of poorly drained soils (Tan et al., 2004). Some wetlands and peat soils present in these areas also contribute to high SOC stocks. Long-term average annual temperature and precipitation data showed lower temperature (<9.3°C) and lower precipitation (900 mm) in areas with high SOC stocks. The SOC stocks were low in MLRAs 114 and 120. These MLRAs are located in the southern part of the state. These areas are mainly situated on steep slopes (>10%) with well-drained mineral soils. Long-term average annual temperature and precipitation are >1100 mm and >11°C, leading to low SOC stocks in these areas. A similar distribution of SOC stocks in these MLRAs was also observed by Tan et al. (2004) in Ohio. The observed effect of precipitation on SOC is consistent with the pattern observed by Guo et al. (2006b) in the conterminous United States, and Burke et al. (1989) in the Central Plains grasslands. These studies suggested fluctuation of SOC content as precipitation increases from 850 mm. The SOC stocks in the entire state of Indiana were estimated to be 0.90 Pg using the predicted SOC stock map from Procedure B.

The spatial variability of SOC stocks obtained from this study was compared with previous studies that used different data sources. Guo et al. (2006a) used the STATSGO database

Table 3. Variogram model parameters fitted using both procedures.

Variable	Model	Procedure A			Procedure B		
		Nugget	Sill	Range	Nugget	Sill	Range
				km			km
Parameter *a*	spherical	294.5	494	52.5	1.42	4.18	69.7
Parameter *b*	spherical	11.7	11.18	52.5	0.075	0.30	28.3

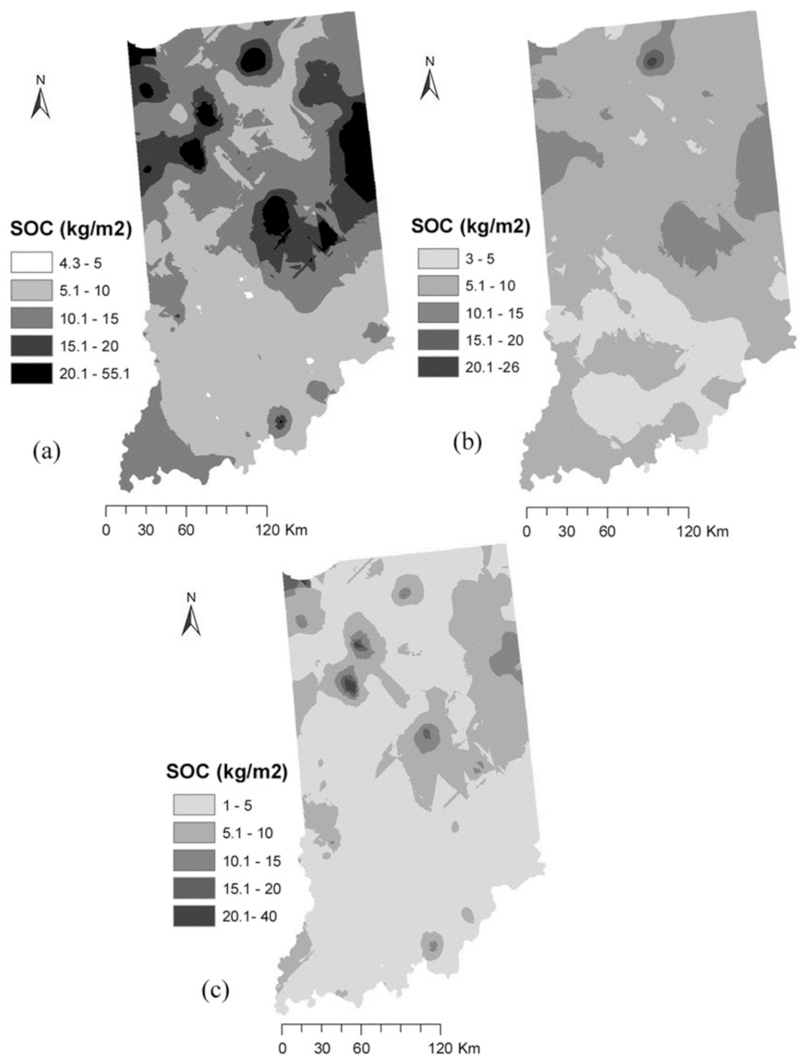

Fig. 5. Predicted soil organic C (SOC) stock maps for (a) 0 to 1, (b) 0 to 0.5, and (c) 0.5 to 1.0 m using Procedure B. Small blank areas in (c) represent the areas with soils <0.5 m deep.

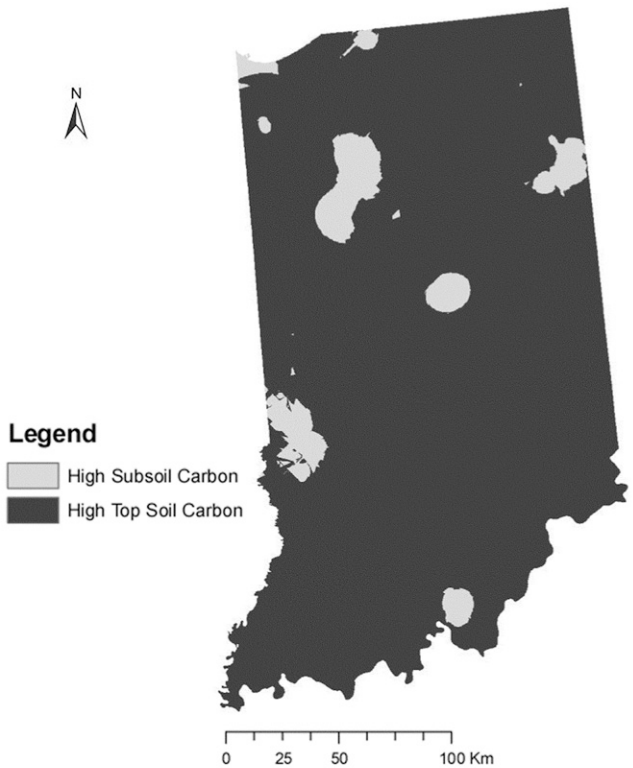

Fig. 6. Regions of high topsoil soil organic C (SOC) and high subsoil SOC in the study area.

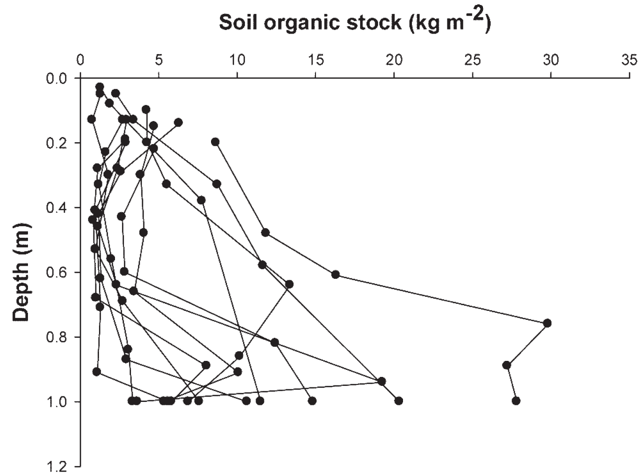

Fig. 7. Profile depth distributions of soil organic C (SOC) stocks of the pedons with higher subsoil SOC stock.

to generate an SOC stock map of the United States. Indiana in the continental SOC stock map of that study showed a similar trend of spatial variability of SOC stocks as in the map presented in Fig. 5a. For instance, the northern part of that map shows higher SOC stocks (>10 kg m^{-2}) than the southern part (<10 kg m^{-2}), which is similar to our results. Likewise, Kern (1994) prepared an SOC stock map of the United States up to 1-m depth using 3700 pedon data. The map of Indiana prepared using the soil taxonomy approach of that study is also similar in most details to the map of Fig. 5a. That map divided Indiana broadly into three main SOC stock regions. The northern portion of the state showed the highest SOC stock of 18.1 to 19.5 kg m^{-2}, which is a comparable result to our map (>20 kg m^{-2}) in this area. The middle portion of the state showed an SOC stock of 12.1 to 13.5 kg m^{-2}, and the southern portion showed the lowest SOC stock of 7.6 to 9 kg m^{-2}. Our results suggest 10.1 to 15 kg m^{-2} and <10 kg m^{-2}, respectively, in these parts of the state. These comparisons further confirm the validity of our results.

Looking at the limitations and possible uncertainties associated with the prediction, this map reflects the C stocks of about two decades ago, as the soil samples were collected in 1975 to 1990. Therefore, the current SOC stocks might have changed due to various management factors. Similarly, the bulk density values were predicted for few pedons, which might create uncertainty in the predictions. Likewise, the study area was not covered uniformly with SOC samples; therefore the SOC stock estimates at sparsely sampled areas will be associated with higher prediction errors.

SUMMARY AND CONCLUSIONS

In this study, the spatial variability of SOC stocks was predicted at three depth intervals within the upper 1-m depth on a state scale using the profile depth distribution and ordinary kriging. The SOC stock map of this study shows comparable variability of SOC stocks to previous studies conducted in this region using other data sources. Therefore, predicting parameters based on exponential soil depth functions is a time- and cost-saving approach to estimating and mapping SOC stocks at larger spatial scales. The validation indices showed that the second method (Procedure B) of fitting the exponential function produced lower estimation errors in predicting the SOC stock. This method of predictive mapping is especially useful where there are missing observations for some horizons, as they can be interpolated using the exponential equations.

Extensive data sets of environmental parameters are becoming increasingly available due to technological improvements in data collection techniques. Such data are likely to support environmental studies where sampling to record the variable of interest is constrained by time and cost factors. Therefore, the use of profile depth distribution and geostatistics is promising to

Table 4. Validation indices of soil organic C stock for 0 to 1 m, topsoil (0–0.5 m), and subsoil (0.5–1.0 m) using both procedures.

Index	Procedure A			Procedure B		
	0–1.0 m	0–0.5 m	0.5–1.0 m	0–1.0 m	0–0.5 m	0.5–1.0 m
r	0.64	0.68	0.34	0.68	0.75	0.50
Mean estimation error, kg m^{-2}	−0.86	−0.10	−1.15	0.70	−0.59	1.27
RMSE, kg m^{-2}	3.93	3.27	2.61	3.73	2.89	2.57

Table 5. Results of a *t*-test used to test the hypothesis that the slope of the regression line equals 1 for 0 to 1 m, topsoil (0–0.5 m), and subsoil (0.5–1.0 m) using both procedures.

Statistic	Procedure A			Procedure B		
	0–1.0 m	0–0.5 m	0.5–1.0 m	0–1.0 m	0–0.5 m	0.5–1.0 m
t statistic	−6.016	−5.301	−15.58	−1.12	−6.33	−0.411
P value	0.0001	0.0001	0.0001	0.1338	0.0001	0.3411

map SOC stocks at different spatial scales (county, state, and region) and for different depth intervals.

ACKNOWLEDGMENTS

This project was funded by U.S. Department of Energy through the MRCSP project led by Battelle, Columbus, OH. U. Mishra appreciates the help of Sheila Christopher and Kemal Gokkaya during field work and Budiman Minasny, Hunter Anderson, and Dhiraj Sharma for suggestions during data analysis.

REFERENCES

Adams, W.A. 1973. The effect of organic matter on the bulk and true densities of some uncultivated podzolic soils. J. Soil Sci. 24:10–17.

Amichev, B.Y., and J.M. Galbraith. 2004. A revised methodology for estimation of forest soil carbon from spatial soils and forest inventory data sets. Environ. Manage. 33:S74–S86.

Batjes, N.H. 1996. Total carbon and nitrogen in the soils of the world. Eur. J. Soil Sci. 47:151–163.

Baxter, S.J., and M.A. Oliver. 2005. The spatial prediction of soil mineral N and potentially available N using elevation. Geoderma 128:325–339.

Blake, G.R., and K.H. Hartge. 1986. Bulk density. p. 363–375. *In* A. Klute (ed.) Methods of soil analysis. Part 1. 2nd ed. Agron. Monogr. No. 9. ASA and SSSA, Madison, WI.

Burke, I.C., C.M. Yonker, W.J. Parton, C.V. Cole, D.S. Schimel, and K. Flach. 1989. Texture, climate, and cultivation effects on soil organic matter content in U.S. grassland soils. Soil Sci. Soc. Am. J. 53:800–805.

Calhoun, F.G., N.E. Smeck, B.K. Slater, J.M. Bigham, and G.F. Hall. 2001. Predicting bulk density of Ohio soils from morphology, genetic principles, and laboratory characterization data. Soil Sci. Soc. Am. J. 65:811–819.

Devore, J., and R. Peck. 1993. Statistics: The exploration and analysis of data. Wadsworth Publ. Co., Belmont, CA.

Eswaran, H., E. Van Den Berg, and P. Reich. 1993. Organic carbon in soils of the world. Soil Sci. Soc. Am. J. 57:192–194.

Goidts, E., and B. van Wesemael. 2007. Regional assessment of soil organic carbon changes under agriculture in southern Belgium (1955–2005). Geoderma 141:341–354.

Grace, J. 2004. Understanding and managing the global carbon cycle. J. Ecol. 92:189–202.

Guo, Y., R. Amundson, P. Gong, and Q. Yu. 2006a. Quantity and spatial variability of soil carbon in the conterminous United States. Soil Sci. Soc. Am. J. 70:590–600.

Guo, Y., P. Gong, R. Amundson, and Q. Yu. 2006b. Analysis of factors controlling soil carbon in the conterminous United States. Soil Sci. Soc. Am. J. 70:601–612.

Hengl, T., G.B.M. Heuvelink, and A. Stein. 2004. A generic framework for spatial prediction of soil variables based on regression kriging. Geoderma 120:75–93.

Homann, P.S., P. Sollins, M. Fiorella, T. Thorson, and J.S. Kern. 1998. Regional soil organic carbon storage estimates for western Oregon by multiple approaches. Soil Sci. Soc. Am. J. 62:789–796.

Intergovernmental Panel on Climate Change. 2007. Climate change 2007: The physical science basis. Cambridge Univ. Press, Cambridge, UK.

Kern, J.S. 1994. Spatial patterns of soil organic carbon in the contiguous United States. Soil Sci. Soc. Am. J. 58:439–455.

Lal, R. 2004. Soil carbon sequestration to mitigate climatic change. Geoderma 123:1–22.

Lal, R., J.M. Kimble, E. Levine, and C. Whitman. 1995. World soils and greenhouse effect: An overview. p. 1–8. *In* R. Lal et al. (ed.) Soils and global change. CRC Press, Boca Raton, FL.

McBratney, A.B., I.O.A. Odeh, T.F.A. Bishop, M.S. Dunabar, and T.M. Shatar. 2000. An overview of pedometrical techniques for use in soil survey. Geoderma 97:293–327.

Meersmans, J., F. De Ridder, F. Canters, S. De Baets, and M. Van Molle. 2008. A multiple regression approach to assess the spatial distribution of soil organic carbon (SOC) at the regional scale (Flanders, Belgium). Geoderma 143:1–13.

Mestdagh, I., P. Lootens, O. Van Cleemput, and L. Carlier. 2004. Soil organic carbon stocks in Flemish grasslands: How accurate are they? Grass Forage Sci. 59:310–317.

Minasny, B.M., A.B. McBratney, M.L. Mendonca-Santos, I.O.A. Odeh, and B. Guyon. 2006. Prediction and digital mapping of soil carbon storage in the Lower Namoi Valley. Aust. J. Soil Res. 44:223–244.

Moran, P.A.P. 1950. Notes on continuous stochastic phenomena. Biometrika 37:17–23.

Multi-Resolution Land Characteristics Consortium. 2006. National land cover database 2001. Available at www.epa.gov/mrlc/nlcd-2001.html (verified 2 Jan. 2009). USEPA, Washington, DC.

National Soil Survey Laboratory. 2006. Soil characterization database. Available online at ssldata.nrcs.usda.gov/ (verified 2 Jan. 2009). Natl. Soil Survey Lab., Lincoln, NE.

Nelson, D.W., and L.E. Sommers. 1996. Total carbon, organic carbon, and organic matter. p. 961–1010. *In* D.L. Sparks (ed.) Methods of soil analysis. Part 3. SSSA Book Ser. 5. SSSA, Madison, WI.

Odeh, I., A. McBratney, and D. Chittleborough. 1994. Spatial prediction of soil properties from landform attributes derived from a digital elevation model. Geoderma 63:197–214.

Post, W.M., R.C. Izaurralde, L.K. Mann, and N. Bliss. 2001. Monitoring and verifying changes of organic carbon in soil. Climate Change 51:73–99.

Post, W.M., and K.C. Kwon. 2000. Soil carbon sequestration and land-use change: Processes and potential. Global Change Biol. 6:317–327.

Post, W.M., T.H. Peng, W.R. Emmanuael, A.W. King, V.H. Dale, and D.L. DeAngelis. 1990. The global carbon cycle. Am. Sci. 78:310–326.

Rasmussen, C. 2006. Distribution of soil organic and inorganic carbon pools by biome and soil taxa in Arizona. Soil Sci. Soc. Am. J. 70:256–265.

Simbahan, G.C., and A. Dobermann. 2006. Sampling optimization based on secondary information and its utilization in soil carbon mapping. Geoderma 133:345–362.

Simbahan, G.C., A. Dobermann, P. Goovaerts, J. Ping, and M.L. Haddix. 2006. Fine resolution mapping of soil organic carbon based on multivariate secondary data. Geoderma 132:471–489.

Sleutel, S., S. De Neve, G. Hofman, P. Boeckx, D. Beheydt, O. Van Cleemput, et al. 2003. Carbon stock changes and carbon sequestration potential of Flemish cropland soils. Global Change Biol. 9:1193–1203.

Soil Conservation Service. 1981. Land resource regions and major land resource areas of the United States. Agric. Handb. 296. U.S. Gov. Print. Office, Washington, DC.

Tan, Z., R. Lal, N.E. Smeck, F.G. Calhoun, B.K. Slater, B. Parkinson, and R.M. Gehring. 2004. Taxonomic and geographic distribution of soil organic carbon pools in Ohio. Soil Sci. Soc. Am. J. 68:1896–1904.

Thompson, J.A., and R.K. Kolka. 2005. Soil carbon storage estimation in a forested watershed using quantitative soil landscape modeling. Soil Sci. Soc. Am. J. 69:1086–1093.

van Groenigen, J.W. 2000. The influence of variogram parameters on optimal sampling schemes for mapping by kriging. Geoderma 97:223–236.

Van Meirvenne, M., J. Pannier, G. Hofman, and G. Louwagie. 1996. Regional characterization of the long-term change in soil organic carbon under intensive agriculture. Soil Use Manage. 12:86–94.

Van Meirvenne, M., and I. Van Cleemput. 2005. Pedometrical techniques for soil texture mapping at a regional scale. p. 323–341. *In* S. Grunwald (ed.) Environmental soil landscape modeling: Geographic information technologies and pedometrics. CRC Press, New York.

Webster, R., and M.A. Oliver. 2001. Geostatistics for environmental scientists. John Wiley & Sons, Chichester, UL.

Yu, D.S., X.Z. Shi, H.J. Wang, W.X. Sun, J.M. Chen, Q.H. Liu, and Y.C. Zhao. 2007. Regional patterns of soil organic carbon stocks in China. J. Environ. Manage. 85:680–689.

Zinn, Y.L., R. Lal, and D.V.S. Resck. 2005. Texture and organic carbon relations described by a profile pedotransfer function for Brazilian Cerrado soils. Geoderma 127:168–173.